Development and microstructure study of closed cell LM13 alloy foams

A thesis submitted in partial fulfillment of
the requirements for the award of the degree of

Master of Technology
(Materials and Metallurgical Engineering)

Under the guidance of

Dr. O.P. Pandey
(Senior Professor)
School of Physics and Materials science

Submitted by

Davinder Singh
Roll No. 601102004

Thapar University, Patiala, (Punjab), INDIA
July-2013

Dedicated to my Parents and my loving sister

CERTIFICATE

This is to certify that Mr. DAVINDER SINGH, Roll No. 601102004 has worked on this thesis report entitled "Development and microstructure study of closed cell LM13 alloy Foams" as a partial fulfillment for award of the degree of MASTERS OF TECHNOLOGY in Materials and metallurgical Engineering. I certify that the matter embodied in this report is of the candidate's own record and not submitted to any other university in any part or full form for the award of such kind of a degree.

25/6/13

Dr. O.P. Pandey
(Senior Professor)
Supervisor
SPMS, Thapar University, Patiala

26/6/13

Countersigned by:

Dr. Kulvir Singh
(Prof. & Head)
School of Physics and Materials Science
Thapar University, Patiala.

Dr. S.K. Mohapatra
Dean of academic Affairs
Thapar University, Patiala

Acknowledgement

With deep regards and profound respect, I avail this opportunity to express my deep sense of gratitude and indebtedness to Dr. O.P Pandey, Senior Professor, School of Physics and Materials Science, for his keen interest, strong motivation and constant encouragement during the course of the work. He always bestowed parental care upon me and evinced keen interest in solving our problems. An erudite teacher, a magnificent person and a strict disciplinarian, I consider myself fortunate to have worked under his supervision.

I thank him for his great patience, constructive criticism and useful suggestions apart from invaluable guidance to me.

I would also like to thank Dr. Kulvir Singh, Professor and Head, School of Physics and Materials Science for his constant guidance and encouragement. I am also thankful to Dr. Puneet Sharma, Dr. B. N. Chudasama, Dr. S.D. Tiwari and all the faculty members of School of Physics and Materials Sciences for their constructive suggestions at different occassions.

It gives me immense pleasure to express my special thanks to Mr. Suresh Kumar and Mr. Ranvir Singh Panwar, who always took keen interest in guiding me during my work.

I would like to convey my sincere gratitude to my friends and colleagues for their support and their timely help and valuable discussions. I owe my sincere thanks to all the staff members of School of Physics and Materials Science for their support and encouragement.

Last but not the least my father Mr. Jarnail Singh and my mother Mrs. Jarnail Kaur are the two guiding pillars of my success, the constant motivation of my parents has been sole source of my inspiration and strength to carry out my work. And above all, I pay my regards to the Almighty for his love and blessings.

(DAVINDER SINGH)

Abstract

Metal foams need no introduction in today's industrial and research sectors. Aluminium foam based components already being used in various engineering applications or are in final stages of development. Prototypes are being made for characterization and testing purposes. The aim of present dissertation is development of closed cell LM13 piston alloy foams. The blowing agent used for foaming of aluminium alloy is $CaCO_3$. Foams are fabricated by varying the amount of blowing agent and at different foaming temperatures. Macroscopic analyses is done by comparing the cell size and cell wall thickness of foam samples developed under different processing conditions.

CONTENTS

Chapter 1 INTRODUCTION 1
1.1 Introduction 1
1.2 Historical Development 2
1.2.1 Pre 90's Era 2
1.2.2 Post 90's era to present 3
1.3 Industrial production 4
1.3.1 ALPORAS Process 5
1.3.2 FOAMCARP Process 5
1.4 Characterization and testing of metal foam 5
1.4.1 Structure of Foam 5
1.5 Properties of metal foam 6
1.5.1 Thermal and electrical properties 7
1.5.2 Mechanical properties 7
1.5.3 Damping and Sound Absorption 7
Chapter 2 LITERATURE REVIEW 10
2.1 Introduction 10
Chapter 3 EXPERIMENTAL DETAILS 25
3.1 Raw Materials 25
3.2 Melting and Foaming of LM13 foam 25
3.3 Characterization 25
Chapter 4 RESULTS AND DISCUSSION 28
4.1 Macroscopic Analysis 28
4.2 Effect of blowing agent 28
4.2.1 Effect on surface morphology of LM13 foam 30
4.2.2 Effect on cell size of LM13 foam 30
4.2.3 Effect on cell wall thickness of LM13 foam 31
4.3 Effect of foaming temperature 32
4.3.1 Effect on surface morphology of LM13 foam 32
4.3.2 Effect on cell size of LM13 foam 33
4.3.3 Effect on cell wall thickness of LM13 foam 34
4.4 Effect of temperature on density 35
Chapter 5 CONCLUSION AND FUTURE SCOPE 37
5.1 Conclusions 37
5.2 Future Scope 37

Index of Tables

Table 1.1: Production methods of foam and their final products [4].....6
Table 3.1: Chemical compositions of LM13 aluminum alloy.....25
Table 3.2: List of Processing parameters with constant heat treatment temperatures.....26
Table 3.3: List of Processing parameters, at different heat treatment temperatures.....27
Table 4.1: Density, foaming efficiency and average pore size and cell wall thickness of foam produced at 850°C.....28
Table 4.2: Density, Foaming Efficiency and Average pore size and cell wall thickness of foam produced with 2 wt.% of $CaCO_3$.....28

Index of Figures

Figure 3.1: Electric Resistance Furnace used for Al foam production.....26
Figure 3.2: Graphite impeller used for melt stirring(Side view).....26
Figure 3.3: Graphite impeller used for melt stirring(Bottom view).....26
Figure 4.1: Macroscopic image of aluminum foam with (a) 1.5wt.% (b) 2wt.% (c) 2.5wt.% blowing agent $CaCO_3$ at 850°C.....29
Figure 4.2: Macroscopic image of different cell size of aluminium foam with variation in amount of blowing agent $CaCO_3$ at 850°C (a) 1.5wt.%, (b) 2wt.% and (c) 2.5wt.%. 31
Figure 4.3: Macroscopic image of aluminium foam showing variation in thickness of cell wall with variation in amount of blowing agent $CaCO_3$ at 850°C (a) 1.5wt.%, (b) 2wt.% and (c) 2.5wt.%. 31
Figure 4.4: Macroscopic images of aluminium foam with 2wt.% blowing agent $CaCO_3$ at (a) 850°C (b) 875°C and (c) 900°C 33
Figure 4.5: Macroscopic image of 2wt.% $CaCO_3$ showing variation in cell wall thickness and node size of the aluminum foams processed at (a) 850°C, (b) 875°C and (c) 900°C.....34

Chapter 1 INTRODUCTION

1.1 Introduction

The field of Porous metals and metallic foams has attracted active research and development activities for many years. Currently around 150 institutions are working on manufacturing and characterization metal foams worldwide [1]. Cellular metals and metallic foams are metals with pores deliberately integrated in their structure. The terms cellular metals or porous metals referring to metals that have large volume of porosities, while the terms foamed metal or metallic foams applies to porous metals produced with processes where foaming take place. The foaming is the process of introducing gas in any liquid phase.

Metal foams are characterized structurally by its cell topology (open cells, closed cells), relative density, cell size, cell shape and anisotropy. The structure of closed- pore foams resembles to a network of soap bubbles and can bear high impact loads. The open-pore foams are identical to the closed-cell ones except there are no cell walls present which produce large channels of interconnected cells. Despite the low structural strength of open cell foams flow-through capability is their main advantage [2].

Metallic foams have combinations of physical and mechanical properties that cannot be obtained with polymer and ceramic foams. For example, the mechanical strength, stiffness and energy absorption of metallic foams are much higher than those of polymer foams. They are thermally and electrically conductive and they maintain their mechanical properties at much higher temperatures than polymers. As opposed to ceramics foams, they have the ability to deform plastically and absorb energy. Their low weight and cellular microstructure endows them with the ability to absorb considerable energy by plastic dissipation under compression [3]. If they have open porosity (open cell foams), they are permeable and can have very high specific surface areas, characteristics required for flow-through applications or when surface exchange are involved. Most of the mechanical properties of foam materials can be achieved with other materials, sometimes more effectively, but foams can offer a unique combination of several (apparently contradictory) properties that cannot be obtained in one conventional material at the same time (e. g., ultra-low density, high stiffness, the capability to absorb crash energy, low thermal conductivity, low magnetic permeability, and good vibration damping). Cellular metals are thus promising in applications where several of these functions required to be combined [4].

The main applications of aluminum foams are found in the automotive industry (impact, acoustic and vibration absorbers), the aerospace industry as structural components in turbines and spatial cones, in the naval industry as low frequency vibration absorbers, and in construction industry as sound barriers inside tunnels and as fire proof materials, structure protection systems against explosions and even as decoration. As far as structural applications are concerned, aluminium foams (pure or with the addition of small quantities of other alloying elements) actually represent the most promising typology owing to their mechanical properties and low cost [5,6].

1.2 Historical development

Polymer foams and rubber materials have been long used as cushions, vibration and sound absorbers, and packaging materials. However their structural applications are very few due to their low strength. In contrast to polymer foams metal foams only started to be used in engineering applications at the beginning of the 20th century and are more stable in harsh environment. Sintered powder and meshes were the first porous metals commercially available and used in engineering applications. Sintered powder has been used with success for the fabrication of filters, batteries and self lubricated bearing since the 1920's. These materials are still in use today in high-volume applications. Metal foams are being called ‘novel materials’ since it seems like that they have been invented recently [7]. But patents from the 1970's or even the 1960's can be found in which many of today’s concepts are already described. Even before 1960's research exists that explains the principles of foaming metals.

1.2.1 Pre 90's era

The earliest mention of metal foam is in a French patent written by author M.A. De Meller in 1925 [8]. Later research was done in 1950's in USA. B. Sosnick in 1948 [9] first developed “foamlike mass of metal”. He first melted a mix of Al and Hg in a closed chamber under high pressure. After releasing of pressure Hg vaporized at the melting temperature of Al and to the formation of a foam occured. In 1951, John C. Elliott of the Bjorksten Research Laboratories (BRL) files a patent describing an improved version of De Meller’s process [10,11]. He proposed to use TiH_2 or ZrH_2 as a blowing agent (BaH_2, LiH, $LiAlH_4$, $CaCO_3$ and other compounds are also claimed to work). Blowing agent is any compound (mostly in powder form) that releases gas at high temperature. The blowing agent (0.5 – 10 wt.% if using hydride) was added to a range of Al-Mg alloys either directly or after having been encapsulated in a low melting eutectic Mg- Zn alloy to avoid excessive oxidation or even burning.

Beside Elliott, William Stuart Fiedler, Stuart O. Fiedler (W.S.' father) and Johan Bjorksten published more than 15 patents in the USA. Some of those describe the design of a continuous foaming process [12]. First at BRL, later at the Lor Corporation the metal foam business is shifted for upscaling and commercial development around 1960.

In 1967 J.A. Ridgway wrote the first patent about stabilizing effect of high melting temperature particles (added to different precursors made of Sn, Ag, Mg and Fe) on metal foam [13]. The stability of aluminum foams can be increased by increasing the melt viscosity or thickening. Several inventions were published in the late 60's to early 70's based processes doing the same. Notable mentions is of L.G Graper's patent that explained stabilizing effects of oxide. During the stirring of melt the atmospheric oxygen converts the blowing agent particles TiH_2 to TiO particles while hydrogen is being liberated [14]. These oxide particles then stabilize the foam. This finding explains why foams were stable although no stabilization measures were taken in past. It was observed that in the absence of oxygen and without any stabilizing agent, substantially no foaming is obtained [14]. MnO_2 was proposed to add to the aluminium alloy melt, which reacts with Al and leads to the formation of alumina particles that are dispersed in the melt. The largely increased density of particles allows one to reduce the amount of blowing agent needed to 1/8 the amount needed for unstabilized melts and also provides more nucleation sites for bubbles. This leads to a more uniform distribution of more and smaller bubbles compared to the destabilized foam. In late 1960, Currie B. Berry of Ethyl Corporation in Baton Rouge proposes thickening the metallic melts to be foamed by sparging oxygen, air or CO_2 through them [15]. Work on metal foams at the Ethyl Corp. ends in the mid 1970s. In 1976 slowing down the decomposition time by oxidizing the surface TiH_2 and ZrH_2 blowing agent S.E. Speed [16] successfully produced aluminum foam with adding the oxidized hydrides to the melt heated just above its liquidus temperature.

The Shinko Wire Co. Ltd., Osaka, Japan, a subsidiary of Kobe Steel, filed a patent of metal foam under trade name 'ALPORAS' in 1985 in Japan and later in Europe and the USA [17,18]. According to this patent metallic Ca (0.2-8%) is added to molten aluminum alloy and stirring is done. During stirring viscosity is increased and after a definite level is obtained TiH_2 (1-3%) is added. After this, the melt is left for foaming for ~15 min [19].

1.2.2 Post 90's era to present

Extensive worldwide research activities on metal foam started in 1990's, which are still ongoing. The main challenge of recent research is to achieve a uniform cellular structure, to perfect the reproducibility in manufacture and to control foam architecture. Metal foams are currently available

commercially under different trade name for example; Alporas, Cymat, Foamcarp, MetComb, Alcan, Hydro.

The milestones in development of metal foam during past 20 years are as follows: Baumeister et al. in 1991 [20] filed a patent in Germany later in Europe and the USA about the development of aluminium foam sandwiches (AFS). These AFS can be used in chassis of any automobile. In 1998 CYMAT Built the world's first commercial SAF (Stabilized Aluminum Foam) casting line. Simultaneous development of foam was being done in Japan and full production was started under the trade name ALPORAS by 2000. Around same time Simancik et al. in 2000 [21] introduced a dimensionally accurate foam under the trade name ALULIGHT. Further research was done extensively on various applications of AFS at Fraunhofer-Institute for Applied Materials Research, Germany [22]. For in situ monitoring of foam Stanzick and Banhart of Fraunhofer-Institute for Applied Materials Research, Germany introduced an x-ray mechanism. Presently x-ray radiography is one of the most important technique for characterization of Foam. Foamtech Co. Ltd. Started production of foamed metals and ecofriendly materials. In 2002 Fritz Michael Streuber filed a patent explaining process for joining the foams. Honda Motor Co., Ltd. filed patents [23] in the year 2006 and 2008. They coated foaming agent with SiO_2 to improve the wetting properties of the same. By the year 2007, BMW had already made prototypes of some of their automotive parts [24]. ERG Aerospace corporation produce metal foam for various applications under trade name DURACEL. The publicly acknowledged applications of metal foam can be found in Audi, Bentley, and Ferrari. Further development in the field of cellular metals are coming every day.

1.3 Industrial production

Metal foams are being made commercially by two processing routes liquid or solid state processing. In solid state route, powdered metal and powdered titanium hydride or zirconium hydride is mixed, pressed and then heated to melting point of metal to decompose hydride, release hydrogen as a gas and produce foam. Alternatively, a slurry of metal powder mixed with foaming agent in an organic adhesive is mechanically agitated which is then heated to give porous metal [1].

In liquid state processing molten metal and stabilizing particulates with foaming agent are mechanically agitated to to produce foam. Liquid metals can also be infiltrated around granules which are then removed. Other more sophisticated methods involve electroless, electrochemical or Chemical vapor deposition of metal onto an open cell polymer foam. A summery of production methods of foam are given in Table 1.

1.3.1 ALPORAS Process

In ALPORAS process, aluminum foam is made from molten aluminum by stabilizing bubbles in the melt. To stabilize the bubbles it is necessary to increase the viscosity and prevent the bubbles from floating. Miyoshi et al. [2] used 1.5 wt.% Ca as a thickening agent. Ca is admixed with molten aluminum at 680°C and stirred for 6 min in an ambient atmosphere. The thickened aluminum alloy is poured into a casting mold and stirred with a blowing agent of 1.6 wt.% TiH_2 at 680°C. After stirring, the molten material is cured for about 15 min, where it expands and fills up the mold. The foamed molten material is then cooled in the mold with a powerful blower.

1.3.2 FOAMCARP Process

Calcium carbonates based foams are available in the market under the trade name FOAMCARP. Gergely et al. [25] used duraclan type metal(Al–9Si–0.5Mg, with a max. of 0.2 wt.% of Cu, Mg and Ti) with 10 vol.% of SiC particulate is melted in induction furnace at 650°C. After 10 secs of stirring, the foaming agent/ Al-12Si powder mixture (1:2 mass ratio) was introduced into the melt and the melt was stirred (at approximately 1200 rpm) for a further 40–90 secs. A low porosity precursor block, with a thickness of about 20 mm, was produced by casting the semi-solid composite into a room temperature mould. The amount of incorporated carbonate was 3.5 wt.% of the composite mass. Precursors thus formed were heated upto 750°C for 15 minutes that lead to thermal decomposition of the foaming agent and the evolved gas (CO_2) foamed the melt.

1.4 Characterization and testing of metal foam

1.4.1 Structure of foam

Foam can structurally be divided not only into open cell or closed-cell foam, rather it can be characterized at different levels of observation: the geometric architecture of the solid (skeleton) in the individual cells and their three dimensional arrangement, the variation of that architecture within a considered sample or part (degree of uniformity), and the microstructure of the solid itself and its surface [5]. Various basic techniques used for characterizing metal foam are optical microscopy, X-ray analysis and SEM analysis. In situ X-ray radiography is done to visualize the bubble formation in the melt.

Mechanical testing of metal foam is done to ensure stability of foam under working conditions. Further tensile, compression, impact, ballistic, fatigue and wear tests can be done.

Table 1.1: Production methods of foam and their final products [4].

Foaming Route	**Direct foaming of melt**			**Indirect foaming via remelting of precursor**	
Process Name	ALPORAS	ALCAN/ HYDRO/ METCOMB	GASAR/ LOTUS	FORMGRIP	ALULIGHT/ (IFAM)
Dominant stabilization factor	Oxide formation in melt	Ceramic added to the melt	Viscosity of eutectic melt	Ceramic added to the melt	Oxides in compacted powder
Gas source	Blowing agent	External gas source	Dissolved gas	Blowing agent	Blowing agent

1.5 Properties of metal foam

Foaming dramatically extends the range of properties of metals. These physical, mechanical, and thermal properties are usually measured by the same methods as those used for dense solids. It is clear that not all properties will change in the same way [5]. Some main properties that do not change are crystal structure, thermal expansion coefficient. melting temperature (solidus-liquidus range).

Other physical properties, such as the heat capacity, are typically linear functions of the density. More specifically it is the sum of the heat capacity of each phase multiplied by its weight fraction. Even in low density metallic foams the weight fraction of gas is small, so that the specific heat of the cellular structure is essentially equal to that of the parent metal. Finally, there are many properties that depend on the density (or porosity) not only linearly, but also on the geometrical structure or the microarchitecture of the cellular structure: the stiffness, the mechanical strength, the thermal and electrical conductivity as well as acoustic properties. Measurement of density of any material is done by weighing a sample and calculating its volume. The most important feature of foams is the relative density (ρ_{rel}) that is, the apparent density of the foam (ρ), divided by the bulk density of the material (ρ_0) from which the foam is made of [2].

The parameters that influence the structure-sensitive properties of cellular metals are (ordered by their importance):

- Intrinsic properties (properties of cell wall material),
- Relative density,
- Type of cellular structure (open or closed cells),

- In a closed-cell foam, the fraction of the solid contained in the cell nodes and edges,
- Irregularity or gradients in mass distribution,
- The cell size and size distribution (including exceptional sizes),
- Shape of the cells and the anisotropy of cells (including exceptional shapes),
- Connectivity of cell edges,
- Defects, by which we mean buckled or broken cell walls.

1.5.1 Thermal and electrical properties

The conduction of heat in closed-cell metal foams occurs mainly through the solid part of the foam. The contribution of the gas, radiation across the pores, and convection within the cell play a minor role. Therefore, the thermal conductivity of foam should be less than its solid counterpart. The conductivity of the cellular metal should be equal to the conductivity of the dense solid times its volume fraction multiplied by an efficiency factor, which is given by the geometry and takes into account the tortuous path of the heat flow. If we assume that a variation of the relative density is caused by a proportional change of the thickness of the cell wall and struts, or an increase of the size of the cells maintaining the cell wall thickness the efficiency factor should be constant. Electrical conduction is also hindered by presence of gas pores and behave in same manner as that of thermal conductivity.

1.5.2 Mechanical properties

In contrast to thermal and electrical properties, the influence of the density and the architecture of the cellular metal on the mechanical properties is much stronger and more complex. For load bearing structures, packaging, and crash elements their importance is evident, however, for functional applications, for example, heat- exchange systems, damping, and filtering the structural stability is also essential [5].

In compression, cellular metals show a unique stress-strain response with a plateau region in which the stress is nearly constant over a wide range of strain. This behavior makes cellular metals interesting for energy absorbing applications where at a relatively low constant stress a large amount of deformation can be absorbed.

1.5.3 Damping and sound absorption

If the structure is subjected to external excitations by sound waves or by mechanical vibrations, the sound can be transmitted or even born by the structure itself. This is most important in the cases,

when the structure oscillates at its resonant or eigen frequencies. The amplitude of the structure acoustic response and hence the sound radiation can be dramatically reduced by increasing the damping of the structure. The rate of vibrational dissipation or the damping in the structure can be characterized by the loss factor. Loss Factor depend upon damping capacity of material which can be defined as energy dissipated in a complete cycle. The typical structural materials with high strength (for example steel, cast iron, aluminum alloys) have unfortunately very little damping. On the another hand, the high damping materials, such as lead, rubber, or soft plastic, have little strength and cannot be regarded as structural materials. The cellular metals exhibit at least one order of magnitude higher values of the loss factor. The dissipation of the vibrations mainly results from the friction between the attaching surfaces of the cracks appearing in the structure and partially due to the vibration of the thin pore walls. Thus, the damping can be enhanced by the reduction of the cell-wall thickness or/and by introducing of imperfections into the structure. Higher loss factor values are therefore obtained with for example foams made of casting aluminum alloys, which can be prepared with very thin cell walls and contain a lot of cracks. If the nonsoluble ceramic particles, for example SiC, Al_2O_3, or graphite are additionally introduced into the structure of metallic cell walls, the damping will be further improved [5].

For sound absorption purposes highly permeable materials such as open-cell polymer foams and glass or mineral wool fibers are generally used. Flammability and evolution of toxic gases when subjected to excessive heat is the main disadvantage of polymer foams. On the other hand fibrous materials are very sensitive to erosion by shedding or fraying especially under the effects of air flow or vibration. Both type of absorbers usually require various facing materials in order to improve durability or to protect the absorber from contamination. Accordingly, the main parameter for good sound absorption is the permeability of the absorber. Therefore, cellular metals can be used for this purpose only if they meet this fundamental requirement. The closed-cell metallic foams are too stiff to convert sound energy into heat by vibration of their cell walls. To increase the sound absorption of closed-cell foams can be machined that results in rough open-pore surface that slightly improves the sound absorption.

REFERENCES:

1. Louis-Philippe Lefebvre, John Banhart and David C. Dunand, Porous metals and metallic foams: Current status and recent developments, Advanced Engineering Materials, (2008), 10, 9, 775-787.

2. Amol A. Gokhale, N.V. Ravi Kumar, B. Sudhakar, S. N. Sahu, Himalay Basumatary and S. Dhara, Cellular metals and ceramics for defence applications, Defence Science Journal, (2001), 61, 6, 567-575.
3. L.J. Gibson and M.F. Ashby, Cellular solids: structure and properties, (1997).
4. M.F. Ashby, A.G. Evans, N.A. Fleck, L.J. Gibson, J.W. Hutchinson and H.N.G. Wadley, Metal Foams: A design guide, Butterworth-Heinemann, (2000).
5. H.P. Degischer and B. Kriszt, Handbook of cellular metals: Production, processing, applications, Wiley-VCH Verlag GmbH & Co. KGaA, (2002).
6. Roberto Montanini, Measurement of strain rate sensitivity of aluminium foams for energy dissipation, International Journal of Mechanical Sciences, (2005), 47, 26–42.
7. John Banhart, Light-metal foams: History of innovation and technological challenges, (2013), 15, 3, 82–111.
8. M. A. De Meller, French Patent 615 147, 1926, (1925).
9. B. Sosnick, US Patent 2 434 775, (1948).
10. John. C. Elliott, Method of producing metal foam. USA Patent 2 751 289, 1956 (1951).
11. John. C. Elliott, Metal foam and method for making. USA Patent 2 983 597, 1961 (1959).
12. W. S. Fiedler, Method of making metal foam bodies. USA Patent 3 214 265, 1965 (1963).
13. J. A. Ridgway Jr., US Patent 3 297 431, (1967).
14. L. G. Graper, Method of making metal foam. USA Patent 3 379 517, 1968 (1965).
15. C. B. Berry, Foamed metal, USA Patent 3 669 654, 1972 (1970).
16. S. E. Speed, US Patent, 3 981 720, (1976).
17. S. Akiyama, H. Ueno, K. Imagawa, A. Kitahara, S. Nagata, K. Morimoto, T. Nishikawa and M. Itoh, Foamed metal and method of producing same, European Patent 0 210 803, 1989 (1986).
18. S. Akiyama, H. Ueno, K. Imagawa, A. Kitahara, S. Nagata, K. Morimoto, T. Nishikawa and M. Itoh, Foamed metal and method of producing same, USA Patent 4 713 277, 1987 (1986).
19. Tetsuji Miyoshi, Masao Itoh, Shigeru Akiyama and Akira Kitahara, ALPORAS Aluminum foam: Production process, properties, and applications, Advanced Engineering Materials, (2000), 2, 4, 179-183.
20. Joachim Baumeister and Hartmut Schader, Method for manufacturing foamable bodies, US5151246, (1991).
21. Frantisek Simancik, Walter Rajner, L.P. Rainhard Laag, Alulight: Aluminum Foam for

Lightweight Construction, SAE 2000 World Congress, (2000).
22. Joachim Baumeister, John Banhart and M. Weber, Aluminium foams for transport industry, Materials & Design, (1997), 18, 4–6, 217–220.
23. Ryoichi Ishikawa, Takashi Nakamura and Katsuhiro Shibata, Honda Motor Co. Ltd., USA patent US7410523 B2, (2006)
24. John Banhart, Aluminium foams for lighter vehicles, International Journal of Vehicle Design, (2007), 37, 2/3.
25. V. Gergely, D.C. Curran and T.W. Clyne, The FOAMCARP process: foaming of aluminium MMCs by the chalk-aluminium reaction in precursors, Composites Science and Technology, (2003), 63, 16, 2301–2310.

Chapter 2 LITERATURE REVIEW

2.1 Introduction

The growing interest towards metal foams has led to rapid development of different process-routes. Metal foams have been obtained starting for different metals like Mg, Al, Cu, Zn, Ti, Fe, Au [1]. They are prepared by direct foaming of the melt or by powder metallurgical (PM) techniques [2]. In some cases introduction of gas into a melted metal which leads to a light metallic structure is produced. A blowing agent generally powder of hydrides, carbonates and nitrides that release gas(usually H_2 or CO_2) at high temperature is used to get foam. Limitations of the use of TiH_2 (e.g. cost, fire risk, harmful H_2 gas) on final foam has stimulated new research on the use of the carbonate decomposition mechanism to achieve foams by PM or melt route. In the recent works the use of $CaCO_3$ was found to be potentially suitable as a blowing agent [3,4]. A cell face stabilizing mechanism operating in carbonate-foamed melts was reported, where $CaCO_3$ acts in contact with molten aluminium as a foaming agent. Further, analysis describing various development stages of metal foam over the years is given below.

František et al. in 1997 [5] studied the formation of aluminium foam which essentially spherical and closed pores occupy more than 70% of the total volume. Mechanical and physical properties depend strongly on the density which lies typically in the range of 0.4-1.2 $g.cm^{-3}$. They have shown that aluminium foam prepared by powder metallurgical method is very efficient in sound absorption, electromagnetic shielding, impact energy absorption and vibration damping.

Banhart et al. in 1998 [6] mentioned that the uniaxial compression of the stress-strain diagram of metal foam depends on the density of the foam, on the relative orientation of the testing and foaming direction, and on the orientation of closed outer skins. Higher densities in general lead to higher stresses under compression conditions but also to a reduction of the range of the technologically important plateau regime. A parallel orientation of the outer skins with respect to the applied force leads to a higher strength and to an extension of the plateau regime as compared to the perpendicular orientation. The relative orientation of force and foaming direction, however, is of minor importance. The foams investigated were therefore nearly isotropic.

Gergely et al. in 1999 [7] reported the stability of liquid metallic foams during preparation of aluminium foam. The fabrication route involves infiltration of the spaces between ceramic layers with expanding semi-liquid metal foam. Examination of the foam macrostructure revealed that cell coarsening is very sensitive to the foam baking parameters (temperature and time). Theoretical

analysis of material redistribution in the liquid foam showed that foam stability can be improved by increasing the melt viscosity. However, analysis suggests that the size of particles should be kept reasonably small to get higher life.

Yanga et al. in 2000 [8] examined the factors which affect the foaming in a foamed aluminum casting process. Proper controlling of holding temperature and titanium hydride content of the melt lead to the production of foamed aluminum. Addition of 1% titanium hydride at 640°C, has produced uniform size of 2 to 6 mm diameter with 86% porosity.

Stanzick et al. in 2000 [9] and Zitha in 2001 [10] analysed the formation process of metal foam under different conditions and analyzed them by different modern techniques.

Banhart in 2001 [11] during his work classified the various manufacturing processes. Liquid metal can be foamed directly by injecting gas or gas-releasing blowing agents, or by producing supersaturated metal–gas solutions. Indirect methods include investment casting, the use of space holding filler materials or melting of powder compacts, which contain a blowing agent. If inert gas is entrapped in powder compacts, a subsequent heat treatment can produce cellular metals even in the solid state. Finally, metal vapour deposition also allow for the production of highly porous metallic structures. The various application fields for cellular metals were discussed.

Kováčik et al. in 2001 [12] experimentally measured the electrical conductivity of Al and Zn based foams prepared by powder metallurgical route with the porosity in the range of 60% - 90% and modeled by means of percolation theory. They observed that electrical conductivity of metallic foams depends predominantly on the electrical conductivity of the matrix metal or alloy and the foam density. The characteristic exponents obtained experimentally was found lower than the theoretically predicted value due to the effect of sample size, surface skin, heterogeneity of foam structure, and the setting of the percolation threshold to zero. The effects of surface skin, heterogeneity of the structure and sample size were further demonstrated.

Simančík et al. in 2001 [13] proposed that the aluminium foams prepared by PM-techniques are very promising materials for lightweight stiff body structures and crash absorbing elements. However, their surface skin usually contains small holes or even cracks which can initiate premature fracture of the foam, especially when they appear on the tensile loaded surface. Strengthening of surface skin with various reinforcements solved this problem effectively.

Nakamura et al. in 2002 [4] employed an established ion-exchange method for the coating of calcium carbonate powder with fluoride for wettability enhancement. Effect of coating was

considered by the examination of wetting behavior of coated and uncoated $CaCO_3$ by the Al melt. It was determined that coated carbonate produced metallic foam with density comparable to that of samples treated by titanium hydride ($\sim 1 \times 10^{-3}$ kg·m^{-3}) and much less then the density of samples obtained by uncoated carbonate (1.7×10^{-3} kg·m^{-3}). It was also observed that coated carbonate ensured aluminum foam with smaller pores (1.1×10^{-3} m) than when the conventional foaming agent, titanium hydride, is used (1.8×10^{-3} m). Their study showed that calcium carbonate is highly applicable to foamed metal production.

Gregely et al. [3] presented a brief outline of the factors that are involved in the search for gas-generating agents offering superior performance for foaming of liquid aluminium alloys. These include kinetic and thermodynamic characteristics of decomposition reactions, the ease of dispersion of the powdered foaming agent in the melt, the nature and likely effect of decomposition products on melt flow, potential reactions, cost and ease of handling of the powder concerned. There is one very promising candidate material, calcium carbonate, which offers advantages compared to currently-employed hydride powders in virtually all aspects of their performance. They found that foams can be produced having appreciably finer cells (<1 mm diameter) and more uniform cell structures than currently available melt route foams, a potentially lower ceramic content in the cell walls and dramatically reduced raw material costs. The presence of an oxidising foaming gas in the cells leads to reaction with the liquid cell surface, forming a continuous oxide film. The presence of this film has a significant effect on foam stabilisation, slowing down cell coalescence and melt drainage.

Heflen et al. in 2005 [14] used Synchrotron-radiation tomography to investigate early foaming stages of aluminium alloys. Monochromatic radiation, high spatial resolution down to the micrometer scale, partial beam coherence, and holographic reconstruction techniques permit the distinction between different foam constituents which are not visible by other volume imaging techniques. In combination with three-dimensional image analysis, the differences in the pore initiation processes in two different aluminium alloys are shown. It was found that, in powder compacts made from prealloyed AA6061 alloy powder, pores appear predominantly around the blowing agent particles whereas, in compacts made from a powder blend of Al and Si, pores tend to initiate around Si particles.

Montanini et al. in 2005 [2] investigated the structural performance of aluminium alloy foams under both static and dynamic compression loads. Three foam typologies (M-PORE, CYMAT, SCHUNK) in a wide range of density (from 0.14 to 0.75 g/cm^3), made by means of different process-routes

(melt gas injection, powder metallurgy, investment casting) were analysed. Microstructure was obtained by SEM and Computed Tomography (CT) and subsequently digital image processing in order to determine average cells size and cell distributions on different section planes. The experimental study aims to assess the mechanical behaviour and the physical and geometrical properties of the foam. They found that the specific energy dissipation of foams with similar density can be quite different: for the same volume of foam, average values of 1770, 1780 and 5590 J/kg at 50% nominal compression have been measured on M-PORE (0.19g/cm^3), CYMAT (0.28g/cm^3) and SCHUNK (0.28g/cm^3) foams, respectively. Impact tests showed that the dependence of the plateau stress on strain rate could be considered negligible for M-PORE and CYMAT foams while it is quite remarkable for SCHUNK foams. Moreover, it was found that the peak stress of CYMAT foams has a quite large sensitivity on the loading rate.

Bryant et al. in 2006 [15] described an alternative processing method for producing aluminum foams. The physical and mechanical properties in these fine (< 1 mm) celled aluminum foams was related to their cellular structure and the properties of the aluminum alloy matrix from which they were produced. Analysis of these materials showed that foam products can be produced over a range of relative densities (7% to 30%) and that average cell diameters can be refined to values of less than 0.5 mm, allowing for the use of the material in thin panel applications. Density of the foam dominates the strength and modulus of the product, following the power law relationship for open cell structures. This relationship breaks down, however, at low densities where the meso-structure and interconnectivity play a more significant role. The fragmentation index may prove to be a useful structural parameter to gauge this interconnectivity and a powerful tool in the development process.

Tzeng et al. in 2007 [16] proposed a modified technique for manufacturing closed-cell aluminum (Al) foams to reduce the cost. The addition of foaming agents promotes the uniformity of cell sizes and controls the viscosity of the melting aluminum alloy. This work elucidated the mechanical characteristics of closed-cell aluminum foams under compressive loading. The thermal conductivity of the aluminum foams was determined and compared with some theoretical predictions. The optimum parameters for meeting some practical design requirements, such as impact absorption and thermal insulation design applications, were discussed. Finally, an empirical correlation between the normalized yield strength and the relative densities was obtained.

Zhu et al. in 2007 [17] reviewed the characteristics of blast loads and corresponding structural response, as well as the current advances in the area of metallic and sandwich structures. Several

critical structural responses were classified and briefly illustrated. The major experimental methods were introduced with a brief description of corresponding experimental devices such as ballistic pendulums and a wide range of sensors to measure impulse, pressure and acceleration and displacement of structures. Several commonly used analytical models were presented and compared to estimate the dynamic behaviour of structure under blast loading. The numerical approaches to analyze the structure responses to blast impact were also summarised with a number of available constitutive relations of explosive charge and material properties of structures.

Banhart et al. in 2008 [18] manufactured sandwich panels consisting of a highly porous aluminium foam core and aluminium alloy face sheets by roll-bonding aluminium alloy sheets to a densified mixture of metal powders, usually Al-Si or Al-Si-Cu alloys with 6-8% Si and 3-10% Cu and titanium hydride, and foaming the resulting three-layer structure by a thermal treatment. Various processing steps of aluminium foam sandwich (AFS), the metallurgical processes during foaming and alternative ways to manufacture AFS (e.g. by adhesive bonding) was reviewed. AFS can be treated two ways after foaming i.e. forging and age-hardening.

Kolluri et al. 2008 [19] conducted an investigation into the constant stress amplitude compression-compression fatigue behavior of closed-cell aluminum foam, both with and without lateral constraint. Results showed that the early stages of strain accumulation due to fatigue loading are independent of constraint, the rapid strain accumulation stage behaviors are sensitive to the constraint. This was ascribed to the noticeable hardening with plastic deformation observed under constraint during quasi-static loading, which in turn reduces the effective maximum stress experienced by the foam specimen during fatigue loading. This was demonstrated through a simple empirical model that connects fatigue strain accumulation without constraint to that under constraint. Complementary X-ray tomography experiments suggest that fatigue behavior of the foams is relatively less sensitive to the morphological defects such as missing walls as the quasi-static mechanical properties such as plastic strength. Evaluation of the energy absorption behavior suggests that the damage that accumulates during fatigue does not affect the energy absorbing ability of the foam adversely.

Dudka et al. in 2008 [20] investigated foaming of aluminium under oxidising and non-oxidising gas atmospheres. Foams were prepared by mixing and pressing Al99.95 and TiH_2 powders and foaming the pressed material in a gas-tight X-ray transparent furnace while following the process by X-ray radioscopy. Structure and distribution of the oxides present in the powders, precursors and foams were studied by light microscopy, scanning and transmission electron microscopy. Sequential

focused ion beam slicing was used to obtain tomographic images of oxide and micropore distributions within the individual cell walls of the foams. A complex hierarchical structure of the oxides was found. Oxides reside in the bulk of the cell walls without a pronounced segregation to the gas/metal interfaces. The presence of air retards foaming due to oxidation of the outer surface.

Cambroneroa et al. 2009 [21] used two calcium carbonate powders as foaming agents on an Al–Mg–Si (AA6061) alloy. Their different characteristics (particle size and chemical composition) modified the manufacturing process to achieve the final foam. AA6061 powders were then mixed with 10% calcium carbonate and, after cold isostatic pressing into green cylinders, hot extruded at different temperatures (475–545°C). The foaming treatment was carried out in a furnace preheated to 750°C using several heating times. The density changed from 2.03 to 2.10 g/cm^3 after cold isostatic pressing to 2.64–2.69 g/cm^3 in precursor materials obtained by hot extrusion. Foaming behaviour depends on the carbonate powder as well as the extrusion temperature. Thus, natural carbonate powder (white marble) produces a foam density close to 0.65 g/cm^3 after a shorter time than when chemical carbonate is used. The foam structure showed a low degree of aluminium draining, no wall cell cracks and a good fine cell size distribution. Compressive strength of 6.11 MPa and 1.8 kJ/m^3 of energy absorption were obtained on AA6061 foams with a density between 0.53 and 0.56 g/cm^3.

Solorzano et al. in 2009 [22] proposed a novel method for measuring the temperature distribution and evolution of metal foams in the molten state. Foamable AlSi9 precursor material containing 0.6 wt.% TiH_2 was foamed, kept at high temperatures and solidified while its temperature distribution was monitored by a thermographic camera. Free foaming and foaming inside a closed mould were carried out and direct and screened IR monitoring were tested. Different heating conditions were applied giving rise to homogeneous and inhomogeneous temperature distributions. The effect of oxidation was studied on a piece of pure aluminium for reference purposes. The error sources of the measured temperature were analysed. Direct monitoring of foams was shown to be associated to serious problems with quantitative temperature measurement, while screened monitoring yielded promising and accurate quantitative results.

Li et al. in 2010 [23] proposed a novel method to fabricate aluminum foam precursor. High viscosity character of semi solid melt as well as stirring technique were used in this method. The blowing agents were homogeneously distributed without adding thicken additions, aluminum foam precursor embedded with distributed blowing agents were fabricated directly and efficiently through this method. Theyinvestigated the effects of main parameters in the fabricating process

such as solid phase fraction, stirring speed, stirring time and stirring blade angle. It was also proved that when solid fraction was lower than 30%, the distribution effects would increase with stirring time and speed. The great amounts of aluminum solid-phases in the semi-solid melt would not lead to more nucleation and harmful initial gas bubbles. The growing behavior of initial gas bubbles in semi-solid melt was closely related to the melt temperature and cluster size of blowing agents. Lower temperature and smaller size of blowing agent cluster were the key factors to better precursors.

Haesche et al. 2010 [24] investigated replacement of TiH_2 as foaming agent by $CaCO_3$ (lime) and $CaMg(CO_3)_2$ (dolomite) for $AlMg_{4.5}$ and $AlSi_9Cu_3$ foams considering influences on foaming capability and cellular structure. Precursor materials were produced from alloy chip and powder mixtures by means of the thixocasting process. $AlSi_9Cu_3$ variants showed expansion levels sufficient for commercial use. Improved performance of dolomite-based foams relies on formation of stabilizing MgO phases, which do not develop during decomposition of $CaCO_3$ in Al-Si-Cu alloys.

Mu et al. in 2010 [25] prepared closed-cell Al–Si foams by molten body transitional foaming process using TiH_2 foaming agent. The cell shape anisotropy ratio of specimens with various relative densities was measured. The quasi-static compressive behavior of Al–Si foams in both longitudinal and transverse directions were investigated. The results show that Al–Si foam loaded in the transverse direction exhibits a lower stress drop ratio. The relationship between plastic collapse stress ratio and cell shape anisotropy is in accordance with Gibson and Ashby model. The plastic collapse stress and the energy absorption property of Al–Si foams increase following power law relationship with relative density. Moreover, Al– Si foams exhibit higher plastic collapse stress and the energy absorption property in the longitudinal direction than that in the transverse direction.

Mukherjee et al. in 2010 [26] studied expansion and contraction phenomena during solidification of liquid metal foams. Such foams were processed by mixing metal powders with TiH_2 powder and compacting the resulting blends, after which the compacted powders were melted. The subsequent foaming process was monitored in-situ by X-ray radioscopy. An intermediate expansion stage during solidification was observed. This solidification expansion (SE) could be linked with phase transformations in the alloy. SE was found to depend mainly on the time spent at the foaming temperature before cooling (holding time), the cooling rate and the alloy composition. The interplay between gas shrinkage, solidification shrinkage, gas production by the blowing agent and gas losses due to out- diffusion was identified as the main reason for SE. While the blowing agent had a major influence on SE, gas dissolved in the metal also played a role, since some SE was observed in

foams blown without TiH_2 by pure pressure manipulation.

Kivorkijan et al. in 2010 [27] investigated the viability of dolomite powder as cost-effective alternative to TiH_2 foaming agent. Closed cells aluminium foam samples were prepared starts from solid, foamable precursors synthesized by powder metallurgy and melt route. Precursors obtained by melt route were machined and additional cold isostatic pressed in order to improve their density. In all cases, the resulted precursors consisted of an aluminium matrix containing various mass fractions of uniformly dispersed dolomite powders of various average particle size and 5wt.% of SiC particulates. Precursors were foamed by inserting into a cylindrical stainless steel mould and placing inside a pre-heated batch furnace at 700°C for 10 min. The quality of foamable precursors was evaluated by determining their initial density and the foaming efficiency. On the other side, the quality of the obtained foams were characterised by their density, microstructure and mechanical properties. Experimental findings confirmed that aluminium foams synthesized with dolomite powder as blowing agent can be prepared by both powder metallurgy and melt route.

Mukherjee et al. in 2010 [28] studied the application of different cooling rates as a strategy to enhance the structure of aluminium foams. The potential to influence the level of morphological defects and cell size non-uniformities is investigated. $AlSi_6Cu_4$ alloy was foamed through the powder compact route and then solidified applying three different cooling rates. Foam development was monitored in-situ by means of X-ray radioscopy while foaming inside a closed mould. The macrostructure of the foams was analysed in terms of cell size distribution as determined by X-ray tomography. Compression tests were conducted to assess the mechanical performance of the foams and measured properties were correlated with structural features of the foams. Moreover, possible changes in the ductile-brittle nature of deformation with cooling rate were analysed by studying the initial stages of deformation. Improvements in the cell size distributions, reduction in micro-porosity and grain size at higher cooling rates was observed, which in turn led to a notable enhancement in compressive strength.

Malekjafarian et al. in 2012 [29] manufactured foamy Al alloy SiCp composites of different densities ranging from 0.4 to 0.7 g/cm^3 by melt-foaming process, which consisted of direct $CaCO_3$ addition into the molten A356 aluminum bath. Mechanical properties and morphological observations indicated that the three-stage deformation mechanism of typical cellular foams is dominant in the produced A356 aluminum foams. Middle-stage stress plateau shrinkage plus compressive strength and bending stress enhancements were observed in denser foams. With the same Al/SiCp ratio, energy absorption ability and plastic collapse strength of the closed- cell foams

were increased with the foam density. Doubling cell-face bending effects resulted in larger compressive than bending strengths in the closed-cell foams; while stiffness lowering was due to the cell-face stretching conditions.

Nandam et al. in 2012 [30] developed in situ composites, where the reinforcing phase was synthesized within the matrix during composite fabrication. The researchers dealt with the processing, microstructural and mechanical characterization of Al–7Si–0.3Mg–10TiB_2 and Al–4Cu–10TiB_2 foams. Composite foams with very low relative density (ρ_{rel} = 0.17–0.37) and foams containing uniform cell sizes were successfully processed. Since the TiB_2 particle sizes are less than 2 μm and have a good wetting behaviour, TiB_2 can be very good foam stabilizers. Microstructural characterization of the cell walls showed significant grain refinement since TiB_2 is a grain refiner. Elemental mapping clearly showed TiB_2 particles at inter dendritic boundaries. Compression testing of the processed foams showed some interesting features. Stress–strain curve showed a lot of serrations which indicated brittle fracture of the cell walls and edges. Hence, it is observed that a balance should be attained between the grain refinement of α-Al grains and the amount of TiB_2 particles to obtain desirable mechanical properties. Energy absorbed by the processed foams was calculated and they were observed to be close to that of the commercially available ALPORAS foams.

Iluk in 2012 [31] investigated the behavior of standalone absorber made of ALPORAS aluminum foam. The limiting parameters in the given foam component are the stability of absorber column and the risk of global buckling. Specimens with different slenderness ratio were crushed in order to find the transition point between local collapse of the cell walls and global buckling of the entire column.

Vesenjak et al. in 2012 [32] reported the behavior of metallic foam under impact loading and shock wave propagation. The main goal of their work was to investigate the material and structural properties of submerged open-cell aluminum foam under impact loading conditions with particular interest in shock wave propagation and its effects on cellular material deformation. For this purpose experimental tests and dynamic computational simulations of aluminum foam specimens inside a water tank subjected to explosive charge have been performed. Comparison of the results shows a good correlation between the experimental and simulation results. The shadowgraph method was used to observe the underwater shock wave formation, propagation and its effects on submerged aluminum foam sample. The average shock wave velocity was determined to be approximately 2,700 m/s. The deformation behavior of submerged aluminum foam sample was not studied in

detail due to insufficient imaging resolution used in experimental testing.

Garcia-Moreno et al. 2012 [33] reviewed the use of X-ray radioscopy for in-situ studies of metal foam formation and evolution. Results demonstrated the power of X-ray radioscopy as diagnostic tool for metal foaming. Qualitative analyses of foam nucleation and evolution, drainage development, issues of thermal contact, mold filling, cell wall rupture and more are given. Additionally, quantitative analyses based on series of images of foam expansion yielding coalescence rates, density distributions, etc., were performed by dedicated software. These techniques help to understand the foaming behavior of metals and to improve both foaming methods and foam quality.

Koizumi et al. in 2012 [34] observed the cell structures to study the shrinkage of aluminum foam produced using carbonates. The cells of foam produced by using dolomite as a foaming agent connected to each other with maximum expansion. It was estimated that foaming gas was released through connected cells to the outside. It was assumed that cell formation at different sites is effective in preventing shrinkage induced by cell connection. The multiple additions of dolomite and magnesium carbonate, which have different decomposition temperatures, were applied. The foam in the case with multiple additions maintained a density of 0.66 up to 700°C, at which the foam produced using dolomite shrank. It was verified that the multiple additions of carbonates are effective in preventing shrinkage.

Byakova et al. in 2012 [35] highlighted the role of foaming agent and processing route in influencing the contamination of cell wall material by side products, which, in turn, affect the macroscopic mechanical response of closed-cell Al-foams. Several kinds of Al-foams have been produced with pure Al by the ALPORAS melt process and powder metallurgical technique, all performed either with conventional TiH_2 foaming agent or $CaCO_3$ as an alternative. Mechanical characteristics of contaminating products induced by processing additives, all of which were presented in one or another kind of Al-foam, have been determined in indentation experiments. Damage behavior of these contaminations affects the micro-mechanism of deformation and favors either plastic buckling or brittle failure of the cell walls.

Palano et al. 2013 [36] subjected aluminium foam sandwiches to four-point bending fatigue test considering the effect of geometric parameters of panels, such as core and plate thickness, and loading mode, such as arm distance. Fatigue strength curves are expressed in terms of different stress amplitude parameters calculated using an analytical model based on laminated plate classical

theory and a solid finite element method model. Despite, the notable fatigue data scatter, originated by foam intrinsic inhomogeneity, experimental fatigue curves are coherent and allow obtaining unified fatigue curves.

Goel et al. in 2013 [37] developed closed cell aluminium fly ash foam through liquid metallurgy route. They investigated its stress-strain behaviour at different strain rates ranging from 700 s^{-1} to 1950 s^{-1}. The numerical model of split Hopkinson pressure bar (SHPB) was simulated using commercially available finite element code Abaqus/Explicit. Validation of numerical simulation was carried out using available experimental and numerical results. Full scale stress—strain curves were developed for various strain rates to study the effect of strain rate on compressive strength and energy absorption. The results showed that the closed cell aluminium fly ash foam is sensitive to strain rate.

Xia et al. in 2013 [38] prepared closed-cell AZ31-Mg alloy foams by melt-foaming method. Homogenizing heat treatment was applied on the foams and the effects of heat treatment on compressive properties of closed-cell Mg alloy foams were investigated systematically. The results showed that homogenizing heat treatment enhanced the compressive properties in terms of yield strength, mean plateau strength, available energy absorption capacity and ideality energy absorption efficiency of the foams. In addition, homogenizing heat treatment greatly reduced the stress drop rates of the foams. Specimens homogenized at the temperature of 480°C for 24 h possessed good combination of yield strength, compressive stability, available energy absorption capacity and ideality energy absorption efficiency under the present experiment conditions

Kamm et al. 2013 [39] investigated different hydrides that could replace TiH_2 as the hitherto most suitable blowing agent for foaming aluminium alloys were. Hydrides taken from the group MBH_4 (M=Li, Na, K) and $LiAlH_4$ were selected. Foamable precursors of alloy $AlSi_8Mg_4$ were manufactured by pressing blends of metal and blowing agent powders. Powders, precursors and precursor filings were studied by mass spectrometry to obtain the hydrogen desorption profile. Foaming experiments were conducted with simultaneous X-ray radiographic. Two Li-containing blowing agents were found to perform well and can be considered alternatives to TiH_2.

REFERENCES:

1. M.F. Ashby, A.G. Evans, N.A. Fleck and L.J. Gibson, J.W. Hutchinson and H.N.G. Wadley, Metal Foams: A design guide, Butterworth-Heinemann, (2000).

2. Roberto Montanini, Measurement of strain rate sensitivity of aluminium foams for energy dissipation, International Journal of Mechanical Sciences, (2005), 47, 26–42.
3. V. Gergely, D.C. Curran and T.W. Clyne, The FOAMCARP process: foaming of aluminium MMCs by the chalk-aluminium reaction in precursors, Composites Science and Technology, (2003), 63, 16, 2301–2310.
4. Takashi Nakamura, Svyatoslav V. Gnyloskurenko, Kazuhiro Sakamoto, Aleksandra V. Byakova and Ryoichi Ishikawa, Development of new foaming agent for metal foam, materials transactions, (2002), 43, 5, 1191-1196.
5. F. Simanèík, J. Jerz, J. Kováèik and P. Minár; Aluminium foam: A new light-weight structural material, Journal of Metallic Materials, (1997), 35(4), 265 – 277.
6. J. Banhart and J. Baumeister, Deformation characteristics of metal foams, Journal of Material Science, (1998), 33, 1431-1440.
7. V. Gergely, F. Simancík, T. J. Matthams and T. W. Clyne, Preparation of ceramic/metal foam laminates using an in situ foaming technique, 12th International Conference on Composite Materials, Paris, France, (Ed: T. Massard), Woodhead, Cambridge. (1999).
8. C.C. Yang and H. Nakae; Foaming characteristics control during production of aluminum alloy foam, Journal of Alloys and Compounds, (2000), 313, 188–191.
9. Heiko Stanzick and John Banhart, Lukas Helfen and Tilo Baumbach; In-situ monitoring of metal foam evolution and decay; Metal foam evolution studied by synchrotron radioscopy, Applied Physics Letters., (2001),78, 1152-1154.
10. P. Zitha, J. Banhart and G. Verbist, Foams, emulsions and their applications, MIT-Verlag Bremen, (2000),13-20.
11. John Banhart, Manufacture, Characterisation and application of cellular metals and metal foams, Progress in Materials Science, (2001), 46, 559–632.
12. J. Kováčik, Š. Barta and J. Bielek, Electrical conductivity of metallic foams, Cellular metals and metal foaming technology, MIT-Verlag (2001).
13. F. Simanèík, Lúèan and J.Jerz, Reinforced aluminium foams, Cellular metals and metal foaming technology, MIT-Verlag (2001), 1-6.
14. L. Helfen, T. Baumbach, P. Cloetens, P. Pernot, H. Stanzick, K. Schladitz and J. Banhart, Investigation of pore initiation in metal foams by synchrotron-radiation tomography, Applied Physics Letters, 86, 231907, (2005).
15. J. Daniel Bryant, Deborah Wilhelmy, Jacob Kallivayalil and Wei Wang, Development of

aluminum foam processes and products, Materials Science Forum, (2006), 519-521, 1193-1200.

16. Sheng-Chung Tzeng and Wei-Ping Ma, A novel approach to the manufacturing and experimental investigation of closed-cell Al foams, The International Journal of Advanced Manufacturing Technology, (2007), 32, 473–479.
17. F. Zhu and G. Lu, A review of blast and impact of metallic and sandwich structures, EJSE special issue: loading on structures, (2007).
18. John Banhart, Hans-Wolfgang Seeliger, Aluminium foam sandwich panels: Manufacture, metallurgy and applications, Advanced Engineering Materials, (2008), 10, 9, 793–802.
19. M. Kolluri, M. Mukherjee, F. Garcia-Moreno, J. Banhart and U. Ramamurty, Fatigue of a laterally-constrained closed cell aluminum foam, Acta Materialia, (2008), 56, 5, 1114–1125.
20. Alexander Dudka and Francisco Garcia-Moreno, Nelia Wanderka and John Banhart, Structure and distribution of oxides in aluminium foam, Acta Materialia, (2008), 56, 15, 3990–4001.
21. L.E.G. Cambroneroa and J.M. Ruiz-Romana, F.A. Corpasb and J.M. Ruiz Prieto, Manufacturing of Al–Mg–Si alloy foam using calcium carbonate as foaming agent, Journal of Materials Processing Technology, (2009), 209, 1803–1809.
22. E. Solórzano, F. Garcia-Moreno, N. Babcsán and J. Banhart, Thermographic monitoring of aluminium foaming process, Journal of Nondestructive Evaluation, (2009), 28.3-4, 141-148.
23. Nan Li, Shuming Xing, Peiwei Bao and Zhimin Liu, A research on fabrication of aluminum foam precursor using semi-solid melt, 2nd International Conference on Mechanical and Electronics Engineering (ICMEE 2010), 1, 49-54.
24. Marco Haesche, Dirk Lehmhus and Jorg Weise, Manfred Wichmann and Irene Cristina Magnabosco Mocellin, Carbonates as foaming agent in chip-based aluminium foam precursor, Journal of Material Science and Technology., (2010), 26, 9, 845-850.
25. Yongliang Mu, Guangchun Yao and Hongjie Luo, Effect of cell shape anisotropy on the compressive behavior of closed-cell aluminum foams, Materials and Design, (2010), 31, 1567–1569.
26. M. Mukherjee, F. Garcia-Moreno and J. Banhart, Solidification of metal foams, Acta Materialia, (2010), 58, 19, 6358-6370.
27. Varuzan Kevorkijan, Sreco Davor Skapin, Irena Paulin, Borivoj Sustaric and Monika Jenko, Synthesis and characterisation of closed cells aluminium foams containing dolomite powder

as foaming agent. Materiali in Tehnologije, (2010), 44, 6, 363-371.

28. M. Mukherjee, U. Ramamurty, F. Garcia-Moreno and J. Banhart, The effect of cooling rate on structure and properties of closed-cell aluminium foams, Acta Materialia, (2010), 58,15, 5031-5042.
29. M. Malekjafarian and S.K. Sadrnezhaad, Closed-cell Al alloy composite foams: Production and characterization, Materials and Design, (2012), 42, 8–12.
30. Sree Harsha Nandam, Nikhil Charbhai, B. S. Murty, S. Sankaran, Microstructural and mechanical characterization of two aluminium based in situ composite foams, Transactions of the Indian Institute of Metals, (2012), 65, 6, 595-600.
31. A. Iluk, Global stability of an aluminum foam stand-alone energy absorber, Archives of civil and mechanical engineering, (2012), 13, 2, 137–143.
32. Matej Vesenjak, Matej Borovinšek, Zoran Ren, Seiichi Irie and Shigeru Itoh, Behavior of metallic foam under shock wave loading, Metals, (2012), 2, 258-264.
33. Francisco Garcia-Moreno, Manas Mukherjee, Catalina Jiménez, Alexander Rack and John Banhart, Metal foaming investigated by x-ray radioscopy, Metals, (2012), 2, 10-21.
34. Takuya Koizumi, Kota Kido, Kazuhiko Kita, Koichi Mikado, Svyatoslav Gnyloskurenko, and Takashi Nakamura, Method of preventing shrinkage of aluminum foam using carbonates, Metals, (2012), 2, 1-9.
35. Alexandra Byakova, Svyatoslav Gnyloskurenko and Takashi Nakamura, The role of foaming agent and processing route in the mechanical performance of fabricated aluminum foams, Metals, (2012), 2, 95-112.
36. F. Palano, R. Nobile, V. Dattoma and F.W. Panella, Fatigue behaviour of aluminium foam sandwiches, Fatigue & Fracture of Engineering Materials & Structures, (2013).
37. Manmohan DASS GOEL, Vasant A. MATSAGAR, Anil K. GUPTA and Steffen MARBURG, Strain rate sensitivity of closed cell aluminium fly ash foam, Transaction of Nonferrous Meterials Society China, (2013), 23, 1080−1089.
38. Xingchuan Xia, Weimin Zhao, Xiangzheng Feng, Hui Feng and Xin Zhang, Effect of homogenizing heat treatment on the compressive properties of closed-cell Mg alloy foams, Materials and Design, (2013), 49, 19–24.
39. Paul H. Kamm, F. Garcia-Moreno, Catalina Jiménez and J. Banhart, Suitability of various complex hydrides for foaming aluminium alloys, Journal of Materials Research, (2013), 2044-5326, 1-8.

Chapter 3 EXPERIMENTAL DETAILS

3.1 Raw materials

Calcium carbonate ($CaCO_3$) is used for the foaming of LM13 piston alloy. LM13 alloy was obtained in the form of ingots. The compositional analysis of the LM13 alloy was done by wet chemical analysis, which is given in Table 3.1 [1].

Table 3.1: Chemical composition of LM13 aluminum alloy

Element	Si	Fe	Cu	Mn	Mg	Zn	Ni	Al
Chemical analysis (wt.%)	12.0	0.4	1.2	0.4	1.00	0.2	1.0	Bal.

3.2 Melting and foaming of LM13 alloy

The LM13 alloy ingot of known weight was melted in a graphite crucible at 725°C in an electric resistance furnace (Fig. 3.1) and stirred at 650 rpm with a graphite impeller (Fig. 3.2 & 3.3). After LM13 alloy was melted, 1.5 wt.% of $CaCO_3$ was poured and stirred until foam begin to rise in the crucible. Impeller was immediately removed from crucible, while the foam was continuously rising up in the crucible. After removal of impeller furnace was closed and temperature was increased to 850°C. Different castings of foam were obtained by following the same route with with different heat treatment temperature i.e 875°C and 900°C. Another batch of casting was produced with different compositions of $CaCO_3$ i.e 2 wt.% and 2.5 wt.%. The processing parameters to develop metal foam are given in Table 3.2 and Table 3.3.

3.3 Characterization

The various foam samples produced with different processing parameters are analysed by taking their photographs with a standard 15 MP camera. Further, micrographs are taken with the help of a Nikon ECLIPSE MA100 optical microscope.

Weight of foam samples is taken by Sartorious GPA5202 weighing machine and volume is calculated from apparent dimension of samples. Density is measured simply by dividing weight and volume.

The foaming efficiency [2] of the precursors is evaluated from the relative density of the foam obtained, ρ_{rel}, calculated by dividing the apparent density of the foam, ρ_F, by the density of aluminium, ρ_{Al}.

Thus, the foaming efficiency is expressed as:

$$\eta = 1 - \rho_{rel} = 1 - (\rho_F / \rho_{Al}) \quad (1)$$

which actually corresponds to the volume fraction of cells in the foam samples.

Table 3.2: List of Processing parameters with constant heat treatment temperatures.

Foam Designation	**Sample 1**	**Sample 2**	**Sample 3**
Melting temperature	725°C	725°C	725°C
Weight of foaming agent($CaCO_3$)	1.5 wt.%	2 wt.%	2.5 wt.%
Foaming Temperature	850°C	850°C	850°C

Figure 3.1: Electric Resistance Furnace used for Al foam production.

Figure 3.2: Graphite impeller used for melt stirring(Side view).

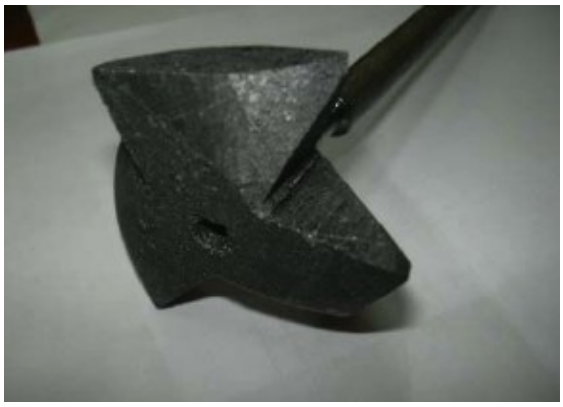

Figure 3.3: Graphite impeller used for melt stirring(Bottom view).

Table 3.3: List of Processing parameters, at different heat treatment temperatures.

Foam Designation	Sample 2	Sample 4	Sample 5
Melting temperature	725°C	725°C	725°C
Weight of Foaming agent ($CaCO_{3)}$	2 wt.%	2 wt.%	2 wt.%
Foaming Temperature	850°C	875°C	900°C

REFERENCES:

1. Ranvir Singh Panwar, O.P. Pandey, Analysis of wear track and debris of stir cast LM13/Zr composite at elevated temperatures, Materials Characterization, (2013), 75, 200–213.
2. Varuzan Kevorkijan, Sreco Davor Skapin, Irena Paulin, Borivoj Sustaric, Monika Jenko, Marjana Lazeta, Influence of the foaming precursor's composition and density on the foaming efficiency, microstructure development and mechanical properties of aluminium foams, MTAEC9 Materials and Technology, (2011), 45, 2, 95–103.

Chapter 4 RESULTS AND DISCUSSION

4.1 Macroscopic Analysis

Metal foam are reviewed at macro level by taking photographs of foam samples after cutting and grinding. Data obtained from these photographs and micrographs is summarized in Table 4.1 & Table 4.2.

Table 4.1: Density, foaming efficiency, average pore size and cell wall thickness of metal foam produced at 850°C

Sample No.	$CaCO_3$ (wt.%)	Morphological properties of obtained Foam			
		Density(gm/cm^3)	Foaming Efficiency(%)	Average pore size (mm)	Cell Wall Thickness (mm)
Sample 1	1.5	0.95	64.8	2.0	1.5
Sample 2	2	0.65	76.0	2.2	1.0
Sample 3	2.5	0.51	81.0	2.3	0.8

Table 4.2: Density, foaming efficiency, average pore size and cell wall thickness of metal foam produced with 2 wt.% of $CaCO_3$

Sample No.	Foaming Temperature (°C)	Morphological properties of obtained Foam			
		Density(gm/cm^3)	Foaming Efficiency(%)	Average pore size (mm)	Cell Wall Thickness (mm)
Sample 2	850	0.65	76.0	2.2	1.0
Sample 4	875	0.55	79.6	2.0	1.2
Sample 5	900	0.86	68.0	1.8	1.4

4.2 Effect of blowing agent

Blowing agents play important role in deciding the pore size. One way for foaming melts is to add a blowing agent directly to the melt instead of injecting gas into it. Heat causes the blowing agent to decompose and release gas, which then propels the foaming process. Table 4.1 indicates density, foaming efficiency, average pore size and cell wall thickness of metal foam produced at 850°C with variation of blowing agent. Figure 4.1(a) shows the effect of variation of blowing agent on the viscosity of aluminum melts at 850°C. The melt soon starts to expand slowly and gradually fills the foaming vessel. The foaming takes place at constant pressure. After cooling the vessel below the

melting point of the alloy, the liquid foam turns into solid aluminum foam and can be taken out of the mold for further processing. An empirical relationship exists between average cell diameter and the viscosity of the melt [1]. The viscosity of molten aluminum can also be enhanced by bubbling gas mixtures through the melt. Metal alloys can be foamed by mixing of foaming agent in the molten mass that releases gas when heated. The widely used foaming agent $CaCO_3$ begins to decompose into CaO and gaseous CO_2, heated from 850°C to 900°C. Large volumes of CO_2 gas produced in molten alloy creates bubbles that can lead to a closed cell foam.

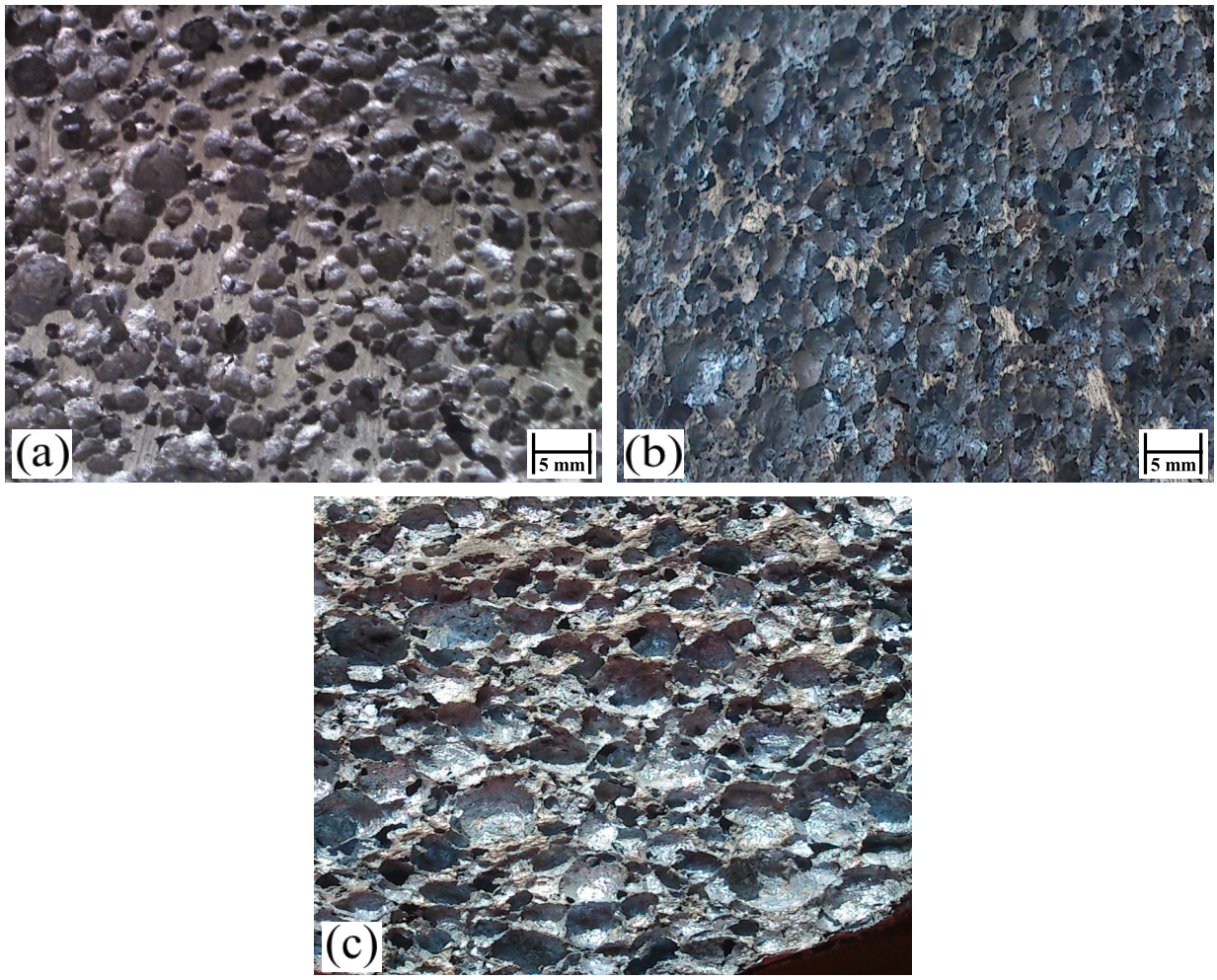

Figure 4.1: Macroscopic image of aluminum foam with (a) 1.5wt.% (b) 2wt.% (c) 2.5wt.% blowing agent $CaCO_3$ at 850°C

The structures of aluminium foam with 1.5wt.% blowing agent $CaCO_3$ is shown in fig. 4.1(a). The optimum temperature for foaming of aluminium lies above the liquidus temperature of the used alloy (850°C). However, the melting temperature of aluminum (660°C) is not sufficient for the proper decomposition of $CaCO_3$ which was used as a foaming agent in this case. At lower foaming temperatures the foaming agent only starts to release less amount of CO_2. The CO_2 gas is inadequate

for the making uniform pore size foam at 850°C (fig. 4.1(a)). With increment in the amount of blowing agent from 1.5wt.% to 2wt.%, an increment in the pore size was observed (fig. 4.1(b)) which is due to large production of CO_2 gas with uniform pore size in molten mass. At 850°C with 2.5wt.% foaming agent is released the large amount of CO_2 gas. This gas expands in the liquid metal and creates lager size bubble like structure. These bubbles are interconnecting to each other as shown in fig. 4.1(c). After decomposition the bubbles formed tries to come out at the surface. Consequently, most of the CO_2 bubbles in the melt meet each other and acquires large area. Under the influence of temperature these unviable bubbles burst on reaching the melt surface. Few stable bubbles ascended to the top surface of the aluminum melt and formed an initial hull of two or three layers of roughly ellipsoidal foam cells [2]. The ensuing foaming caused the shape of the foam cells below the hull to be changed from ellipsoidal to increasingly compressed ones.

4.2.1 Effect on surface morphology of LM13 alloy foam

Figure 4.1(a) shows the closely packed bubbles like structure of the LM13 alloy foam. Foam with a very fine pore structure and some signs of collapse is shown on the some portion in this image. This is due to diffusion of gas from one cell to another which is responsible for the drainage and coarsening of the foam during solidification. Varuzan et al. [3] also observed pores with different diameters that have different internal pressures because pressure is proportional to the inverse of the pore radius, so a smaller pore with a higher pressure disappears after giving its gas to a larger pore. In addition, the membranes between two adjacent cells can rupture spontaneously. Due to drainage and coarsening, there are very large and irregular pores in the middle. Collapsed sections can be seen at the top of the fig. 4.1(a). However, on the left bottom part of the foam in fig. 4.1(b) shows larger number of interconnections between pores, which is due to higher solidification role of foam. The spiral growth inside the pores demonstrate that the gas is released which is a good sign of foaming agent. At 850°C, CO_2 gas expansion make larger size bubble like structure, which is interconnected to each other as shown in fig. 4.1(c).

4.2.2 Effect on cell size of LM13 alloy foam

The cell size of the aluminum foam got increased with increasing rate of CO_2 release. The 1.5wt.% $CaCO_3$ foaming agent results in a much smaller cell size in comparison to the larger cell size produced at 2wt.% and 2.5wt.% $CaCO_3$ foaming agent seen in fig. 4.2 (a, b and c). Consequently most of the air bubbles formed in the melt were large and unstable, and they burst on reaching at the melt surface [4]. This was due to increased size and insufficient strength of the foams under the

increasing weight of the aluminum foam accumulated on top of the aluminum melt. The result was a closely packed bubble like structure of the foam. Therefore, it can be concluded that the increase in amount of foaming agent from 1.5wt.% to 2.5wt.% $CaCO_3$ during the preparation of the aluminum foams has a great effect on the aluminum cell size.

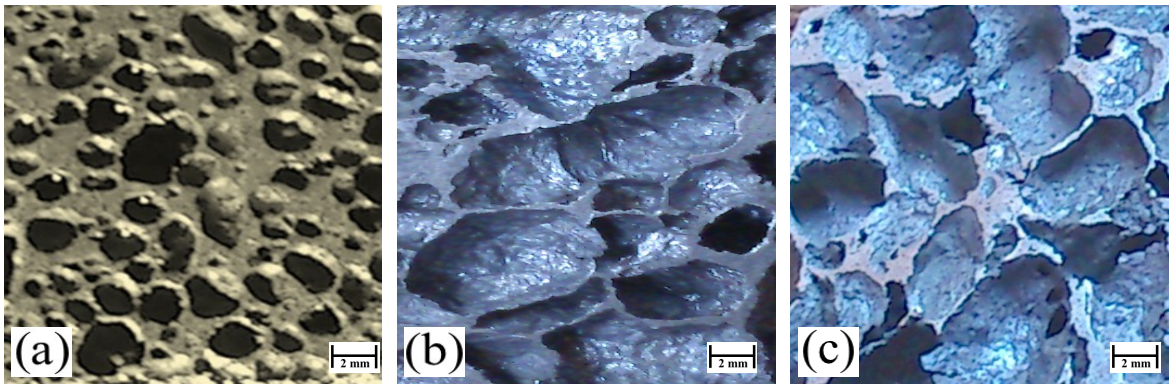

Figure 4.2: Macroscopic image of different cell size of aluminium foam with variation in amount of blowing agent $CaCO_3$ at 850°C (a) 1.5wt.%, (b) 2wt.% and (c) 2.5wt.%.

4.2.3 Effect on cell wall thickness of LM13 alloy foam

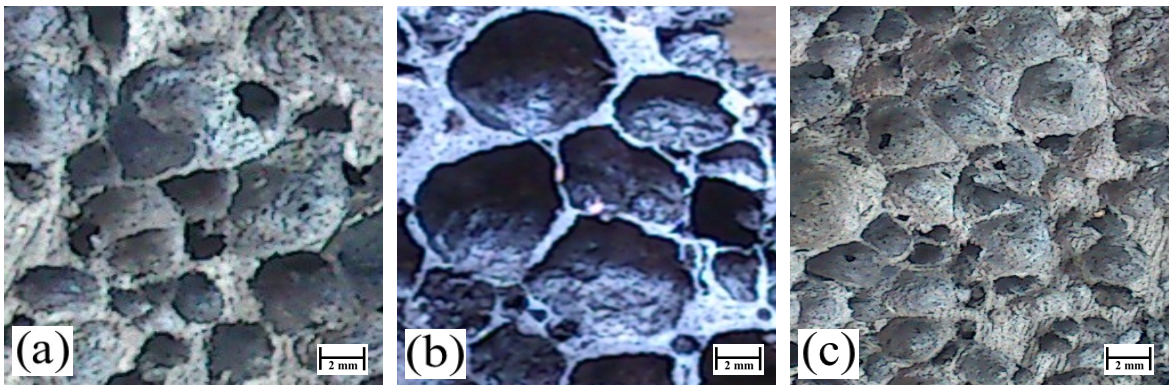

Figure 4.3: Macroscopic image of aluminium foam showing variation in thickness of cell wall with variation in amount of blowing agent $CaCO_3$ at 850°C (a) 1.5wt.%, (b) 2wt.% and (c) 2.5wt.%.

Figure 4.3 (a, b and c) shows the relation of the cell wall thickness and node size versus cell size of the aluminum foams prepared with increasing amount of foaming agent from 1.5wt.% to 2.5wt.% $CaCO_3$. The addition of 1.5wt.% $CaCO_3$ foaming agent in molten metal during the formation of the foam, the cell wall thickness obtained is not uniform. Increment in amount of foaming agent of $CaCO_3$ from 1.5wt.% to 2wt.%, evidently, cell wall thickness and the node size are decreased with the increase in cell size, which is in agreement with Simone and Gibson's study [5] where only the data for mid span of the cell wall is reported. Furthermore, the change in the amount of foaming

agent of ($CaCO_3$) from 2wt.% to 2.5wt.%, seems to have less effect on the cell wall thickness and node size of the aluminum cells. The effect of the higher rate of gas release at 2.5wt.% $CaCO_3$ on cell wall thickness and node size are shown in fig. 4.3(c) where the cell wall thickness and node size are decreased with increasing cell size. The thinner cell wall and node size in contrast with lower rate of gas release at 1.5wt.% $CaCO_3$ observed in fig. 4.3(a) as compared to the higher rate of gas released at 2wt.% and 2.5wt.% $CaCO_3$. This experimental phenomenon comes from the effect of rate of gas release on the size of the closed cell foams.

4.3 Effect of foaming temperature

Table 4.2 summarizes density, foaming efficiency, average pore size and cell wall thickness of metal foam produced with 2 wt.% of $CaCO_3$ at different foaming temperatures. It is observed that less variation in the porosity occurs when the temperature is at 850°C. The cell diameter increases steeply above 850°C. Foaming temperature directly affects the melt surface tension and the foaming agent decomposition. The relationship of melt surface tension and temperature range from 850 to 875°C is calculated as [6]:

$$\sigma = 842 - 0.204\,(T - T_m) \qquad (2)$$

where σ is the surface tension of melt, T is the experimental temperature and T_m is the melt point. Surface tension is known to decrease with increasing temperature, therefore, the stability of the bubble is reduced with increasing temperature. The foaming agent may decompose gas quickly at high temperature [7] and make the experiment too difficult to control. The viscosity decreases and the stability of bubbles reduces at a certain temperature causing increased trend of the bubble mergence and the capacity of the escaped gas, as a result, non-uniform cells can be obtained. At very high temperature foaming agent ($CaCO_3$) disappears due to very fast decomposition, hence very low amount of $CaCO_3$ is available for the mixing in the molten metal. Therefore, the addition of foaming agent should be as much as possible at a relatively low temperature. According to the present investigation, the foaming process ought to be controlled between 850°C and 900°C.

4.3.1 Effect on surface morphology of LM13 alloy foam

During stirring process the $CaCO_3$ charged inside the melt is distributed uniformly inside the melt. The $CaCO_3$ with 2wt.% used as foaming agent decomposes at 850°C to CaO and CO_2 gas. This gas expends the liquid metal and creates bubble like structure. After its formation it tries to come out at the surface. As already mentioned pores with different diameters have different internal pressures because pressure is proportional to the inverse of the pore radius. This explains the signs of collapse

seen on very fine pore structures seen on some portion in figure 4.4(b). This is also due to diffusion of gas from one cell to another which is responsible for the drainage and coarsening of the foam during solidification. In addition, the membranes between two adjacent cells can rupture spontaneously. Due to drainage and coarsening, there are very large and irregular pores in the middle. The $CaCO_3$ with 2wt.% used as foaming agent decomposes at 875°C. Increasing the temperature from 875°C to 900°C, the cell size in the foam is increased as shown in fig. 4.4(c). Figure 4.4(c) reveals that cell size in foam increases with increasing the foaming temperature from 875°C to 900°C. Number of interconnections pores increases with increasing temperature from 850°C to 875°C. However, at 900°C, decrement pore size is observed as shown in fig. 4.4(b).

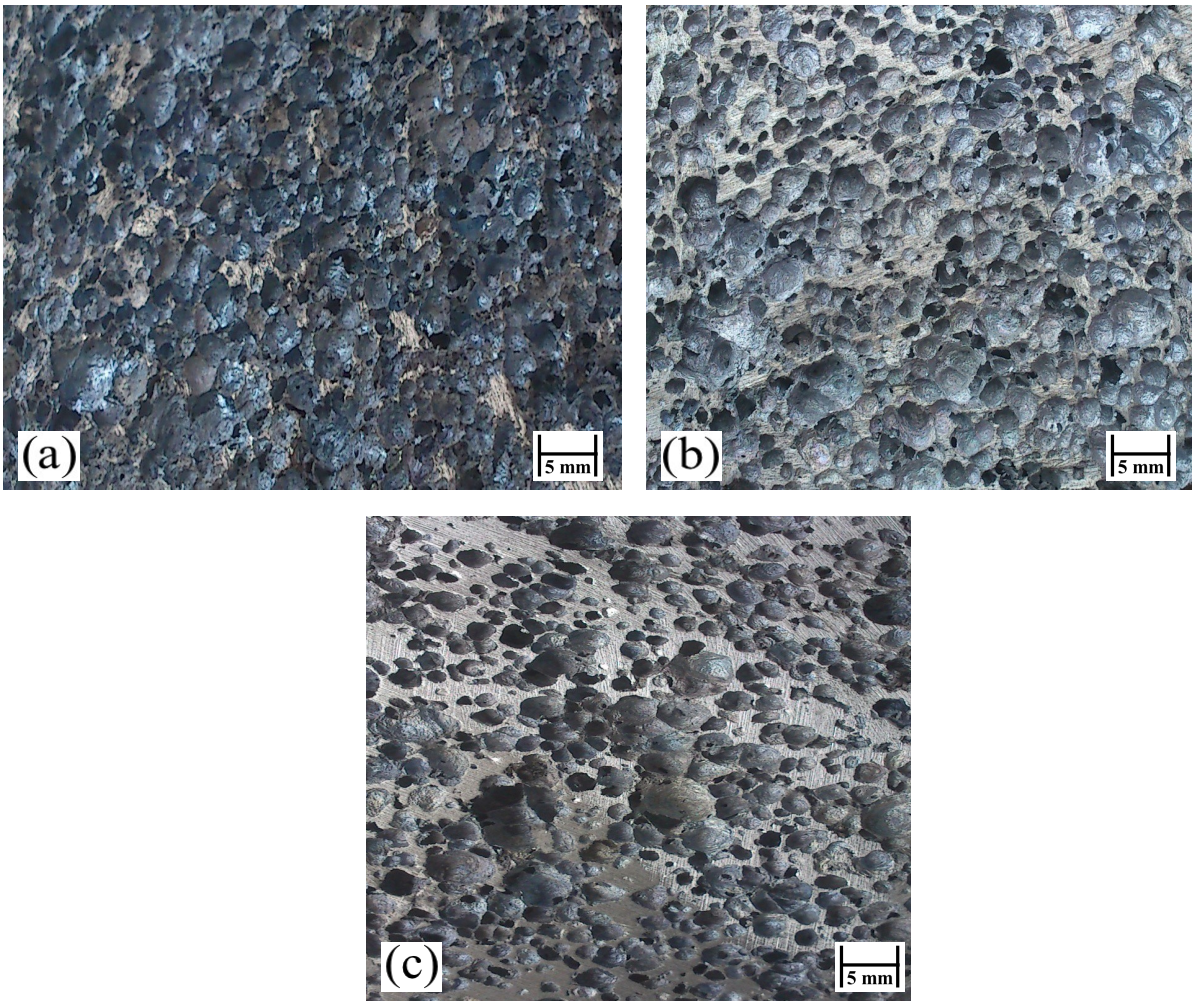

Figure 4.4: Macroscopic images of aluminium foam with 2wt.% blowing agent $CaCO_3$ at (a) 850°C (b) 875°C and (c) 900°C

4.3.2 Effect on cell size of LM13 foam

The effect of the temperature on the cell size of the LM13 alloy foam is shown in fig. 4.4(c). Cell size of the aluminum foam is decreased with increasing temperature from 850°C to 900°C with 2wt.% $CaCO_3$ used as foaming agent. At 850°C with 2wt.% foaming agent results in a larger cell size compared with other temperature (875°C and 900°C). At 875°C, gas bubbles were concentrated at the central part and there was increasing density near the chilled surface. The non-uniformity of distribution and undesirable large size (Fig. 4.4(c)) of some cells have been treated in several ways. Firstly, by using high speed mixing particles of the foaming agent that dispersed throughout the molten metal mass in a very short time. Without exception it was observed that the more uniform is the mixing more uniformity in foam morphology is observed. Secondly, increasing the viscosity of the molten metal can aid in the subsequent blowing step, preventing the escape of bubbles. However, the introduction of a viscosity increasing agent into a molten metal mass is more applicable. Gases produced in molten metal may also acts as a viscosity-increasing agent.

4.3.3 Effect on cell wall thickness of LM13 alloy foam

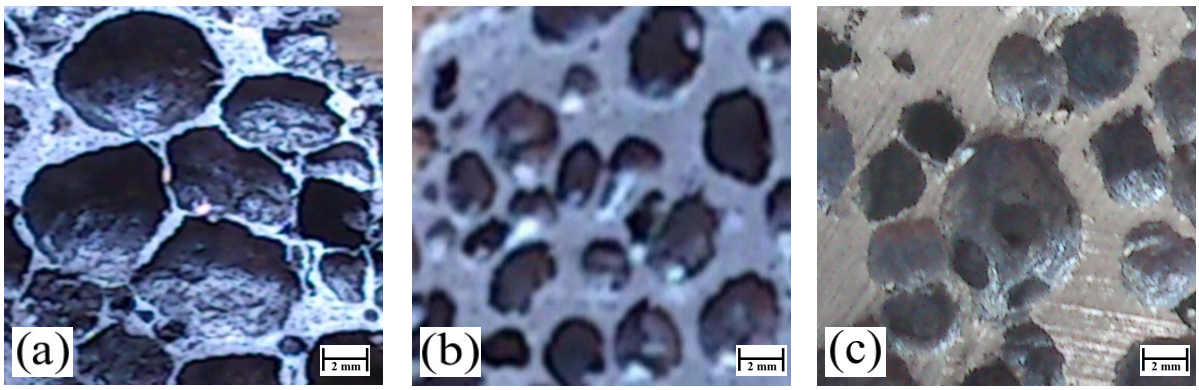

Figure 4.5: Macroscopic image of 2wt.% $CaCO_3$ showing variation in cell wall thickness and node size of the aluminum foams processed at (a) 850°C, (b) 875°C and (c) 900°C

The effect of the temperature on the cell wall thickness of the LM13 alloy foam is shown in fig. 4.5. Cell wall thickness and node size of the aluminum foams are increased with the increase in temperature, and the change of the melting temperature has less effect on the cell wall thickness and node size of the aluminum cells. At 850°C with 2wt.% foaming agent cell wall thickness and node size of the aluminum foams is shown in fig. 4.5(a). At this foaming temperature, alloy slurry is of lower viscosity. As a consequence, the easier drawing of liquid material to cell wall intersections by surface tension causes the thinner cell walls. The change of temperature from 850°C to 875°C, cell wall thickness and node size of the aluminum foams is increased due to the increase in the

temperature, which leads to decrease in viscosity. At 875°C temperature, lower rate of gas release of CO_2 into the melt is completely mixed and create bubbles on the surface of the melt, forming liquid foam. The cell wall thickness of the sample foam is decreased with the increasing the temperature from 875°C to 900°C, as shown in fig. 4.5(b & c). The increase in the thickness of the cell wall at certain temperature implies that the viscosity of the LM13 alloy melt is becoming higher. The air trapped in the liquid foam upon forming at the increased temperatures is responsible for the cell size reduction due to its more expansion which makes the cell wall larger. However, the increase in the cell wall thickness is caused mainly by increasing the viscosity of the LM13 alloy melt.

4.4 Effect of temperature on density

In all cases the experimental results clearly indicate that the foaming efficiency is increasing with respect to increasing the amount of blowing agent. Generally, foamable precursors with a lower porosity resulted in foam samples with a higher apparent density and a lower foaming efficiency. Under the same foaming conditions (foaming agent, temperature), the average pore size of the foam samples was influenced by the density of foaming precursors and the initial size of the foaming particles. Figure 4.5 shows the effects of temperature on the aluminum foam cell size. The porosity continues to decrease with increasing temperature from 850°C to 900°C. The stirring process aims to make the foaming agent particles disperse uniformly, so it is critical to obtain suitable stirring time. Too short or too long stirring time is not suitable to fabricate the uniform size of cell of aluminum foam. Holding is a process of gas growing which effect the pore shape [8]. In the initial period, the gas begins to grow, and the pore is circular shape. When the volume of gas in the melt reaches a certain proportion, the bubbles get crowded. Under the pressure inside the bubble, the melt among the bubbles turns into thin film. According to Laplace's law, the additional surface pressure of the big bubbles is relatively small, when it could not offer enough tension force to keep a big bubble in the sphere, the bubble gives way to the pressure from the melt and becomes a polyhedron, which forms the cellular structure. Based on above analysis, the critical temperature of 875°C, and effective foaming agent (2wt.%) are appropriate for the formation of circular foams.

REFERENCES:

1. John Banhart, Manufacturing routes for metallic foams, JOM, (2000), 52, 12, 22-27.
2. C. Park and S. R. Nutt, Anisotropy and strain localization in steel foam, Materials Science and Engineering: A 299, (2001), 1, 68-74.

3. Varuzan Kevorkijan, Sreco Davor Skapin, Irena Paulin, Borivoj Sustaric, Monika Jenko and Marjana Lazeta, Influence of the foaming precursor's composition and density on the foaming efficiency, microstructure development and mechanical properties of aluminium foams, MTAEC9 Materials and technology, (2011), 45, 2, 95–103.
4. G. Castro and S. R. Nutt, Synthesis of syntactic steel foam using gravity-fed infiltration, Materials Science and Engineering: A, (2012).
5. A. E. Simone and Lorna J. Gibson, Aluminum foams produced by liquid-state processes, Acta materialia, (1998), 46, 9, 3109-3123.
6. Bo Young Hur, Soo Han Park and Arai Hiroshi, Viscosity and surface tension of Al and effects of additional element, Materials Science Forum, (2003), 439, 51−56.
7. Biljana Matijasevic and John Banhart, Improvement of aluminium foam technology by tailoring of blowing agent, Scripta Materialia, (2006), 54, 4, 503-508.
8. Zhen-lun Song, Jin-song Zhu, Li-qun Ma and De-ping He, Evolution of foamed aluminum structure in foaming process, Materials Science and Engineering, (2001), A 298, 1, 137-143.

Chapter 5 CONCLUSIONS AND FUTURE SCOPE

5.1 Conclusions

From the above work following conclusions are drawn:

1. Proper control of the process parameters, such as foaming agent, experimental temperature and stirring and holding time, leads to the production of LM13 alloy foam with a uniform cell structure and high porosity. The average pore size and porosity change little with 1.5wt.%-2.5wt.% $CaCO_3$, while the average pore size and porosity decrease with increasing foaming temperature. LM13 alloy foam with average cell diameter of 2 mm and uniform distribution was obtained under the optimum parameters of the addition of 2wt.% $CaCO_3$ at temperature of 875°C and stirring time and holding time of 5 min and 3 min, respectively.
2. The foaming efficiency of experimentally prepared precursors was evaluated based on the relative density of foams obtained (the apparent density of the foam divided by the density of aluminum). The experimental findings showed that the apparent density of the foam samples is inversely proportional to the density of the foaming precursor.

5.2 Future Scope

In present dissertation only effect of initiation processing conditions on morphology of foam has been studied. This study is required to ensure reproducibility and large scale production of foam. Furthermore, study is to be done on mechanical, thermal, electrical and damping properties of foam to achieve foam that can and are being used various engineering applications. Also, overall incorporation of metal foam (fitting and joining) in engineering components is required.

Contents

Chapter 1 INTRODUCTION 1
1.1 Introduction 1
1.2 Historical development 2
1.2.1 Pre 90's era 2
1.2.2 Post 90's era to present 3
1.3 Industrial production 4
1.3.1 ALPORAS Process 5
1.3.2 FOAMCARP Process 5
1.4 Characterization and testing of metal foam 5
1.4.1 Structure of foam 5
1.5 Properties of metal foam 6
1.5.1 Thermal and electrical properties 7
1.5.2 Mechanical properties 7
1.5.3 Damping and sound absorption 7
Chapter 2 LITERATURE REVIEW 11
2.1 Introduction 11
Chapter 3 EXPERIMENTAL DETAILS 25
3.1 Raw materials 25
3.2 Melting and foaming of LM13 alloy 25
3.3 Characterization 25
Chapter 4 RESULTS AND DISCUSSION 28
4.1 Macroscopic Analysis 28
4.2 Effect of blowing agent 28
4.2.1 Effect on surface morphology of LM13 alloy foam 30
4.2.2 Effect on cell size of LM13 alloy foam 30
4.2.3 Effect on cell wall thickness of LM13 alloy foam 31
4.3 Effect of foaming temperature 32
4.3.1 Effect on surface morphology of LM13 alloy foam 32
4.3.2 Effect on cell size of LM13 foam 33
4.3.3 Effect on cell wall thickness of LM13 alloy foam 34
4.4 Effect of temperature on density 35
Chapter 5 CONCLUSIONS AND FUTURE SCOPE 37
5.1 Conclusions 37
5.2 Future Scope 37

Index of Tables

Table 1.1: Production methods of foam and their final products [4] 6
Table 3.1: Chemical composition of LM13 aluminum alloy 25
Table 3.2: List of Processing parameters with constant heat treatment temperatures. 26
Table 3.3: List of Processing parameters, at different heat treatment temperatures. 27
Table 4.1: Density, foaming efficiency, average pore size and cell wall thickness of metal foam produced at 850°C 28
Table 4.2: Density, foaming efficiency, average pore size and cell wall thickness of metal foam produced with 2 wt.% of $CaCO_3$ 28

List of Figures

Figure 4.1: Macroscopic image of aluminum foam with (a) 1.5wt.% (b) 2wt.% (c) 2.5wt.% blowing agent CaCO3 at 850°C.....29
Figure 4.2: Macroscopic image of different cell size of aluminium foam with variation in amount of blowing agent CaCO3 at 850°C (a) 1.5wt.%, (b) 2wt.% and (c) 2.5wt.%. 31
Figure 4.3: Macroscopic image of aluminium foam showing variation in thickness of cell wall with variation in amount of blowing agent CaCO3 at 850°C (a) 1.5wt.%, (b) 2wt.% and (c) 2.5wt.%. 31
Figure 4.4: Macroscopic images of aluminium foam with 2wt.% blowing agent CaCO3 at (a) 850°C (b) 875°C and (c) 900°C 33
Figure 4.5: Macroscopic image of 2wt.% CaCO3 showing variation in cell wall thickness and node size of the aluminum foams processed at (a) 850°C, (b) 875°C and (c) 900°C.....34